Foam formation in the plastics industry

A. Bradley[1], M. J. Cooker[2], P. J. Dellar[3], A. D. Fitt[4],
A. C. Fowler[5,‡], J. P. Keener[6], J. R. King[7], A. A. Lacey[8],
W. T. Lee[5,‡], S. L. Mitchell[5,‡], G. Richardson[9,‡], M. Vynnycky[5,‡,*]

[1]Department of Mathematics and Statistics, University of Strathclyde,
26 Richmond Street, Glasgow, G1 1XH, Scotland, UK

[2]School of Mathematics, University of East Anglia, Norwich, NR4 7TJ, UK

[3]Oxford University, Mathematical Institute, 24-29 St. Giles', Oxford, OX1 3LB, UK

[4]Oxford Brookes University, Headington Campus, Gipsy Lane, Oxford, OX3 0BP, UK

[5]Mathematical Applications Consortium for Science and Industry (MACSI),
Department of Mathematics and Statistics, University of Limerick,
Limerick, Republic of Ireland

[6]University of Utah, Department of Mathematics, 155 South,1400 East,
Salt Lake City, UT 84112 USA

[7]University of Nottingham, School of Mathematical Sciences,
Nottingham, NG7 2RD, UK

[8]Heriot Watt University, School of Mathematics & Computer Science,
Department of Mathematics, Edinburgh EH14 4AS, Midlothian, Scotland, UK

[9]School of Engineering Science, University of Southampton,
Southampton, SO17 1BJ, UK

[‡]Contributed to the preparation of the report

[*]Corresponding author. E-mail: michael.vynnycky@ul.ie (Michael Vynnycky)

September 24, 2011

Abstract

The manufacture of polyvinyl (PVC) fascia boards involves the extrusion of a pressurized mixture of molten PVC and foaming agents through a die that is shaped in the exterior of a board; subsequent pressure release triggers foaming, so that the interior of the board is filled, simultaneously as the board is cooled. Sometimes, however, the foam does not fill the interior, leading to undesired voids, especially at corners. We consider a mathematical model for the foaming process that attempts to account for the formation of undesired voids. Preliminary model results suggest that severe temperature gradients through the cross-section are most likely responsible for void formation; two mechanisms are suggested.

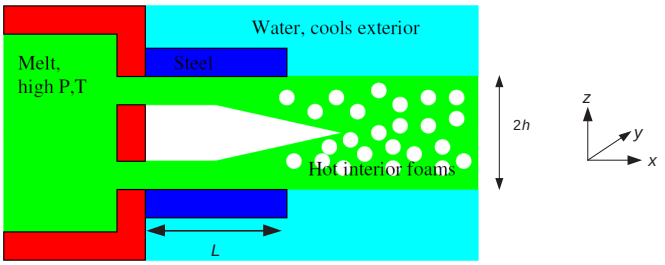

Figure 1: Side view of the foaming process

1 Introduction

Fascia boards, for use on roofs, are often made from foamed polyvinyl chloride (PVC). The fabrication process consists of several steps:

1. A mixture of PVC in the form of fine powder, foaming/blowing agents (azodicarbonamide or oxybis(benzenesulphonylhydrazide) for the the production of nitrogen, and sodium carbonate for the production of carbon dioxide) and sundry lubricants and thermal stabilizers, is heated in a twin-screw extruder by friction and compression, at a typical pressure of 130 bar, to a temperature of around 175°C.

2. The resulting melted material, which has the consistency of chewing gum, is forced through a carefully shaped die, as shown schematically in Figures 1 and 2.

3. On exiting the die, the material undergoes a pressure drop - down to atmospheric pressure - so that the blowing agents which, due to the high pressure within extruder, are held in solution in the melt, turn into a gas and cause the PVC melt to become a foam which quickly expands to fill the void in the centre of the profile.

4. The top of the product is coated with material that gives it a smooth, glossy and weatherable surface.

5. The PVC is then cooled down to solidify the foam from the outside inwards. For the first few centimetres, the outside shape remains in a stainless steel calibrator, so that its shape does not change. It then moves slowly through a cold water bath. Ideally, the foam should completely fill the space at the end of the process.

In the process, the purpose of foaming is to enable as little PVC to be used as necessary, thereby reducing cost: the general aim is to produce a lightweight

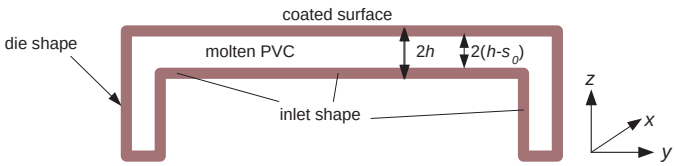

Figure 2: Front-on schematic of the foaming process: the grey region marks the extent of the inlet, and the outer edge of this region coincides with the die shape and the shape of the final fascia board

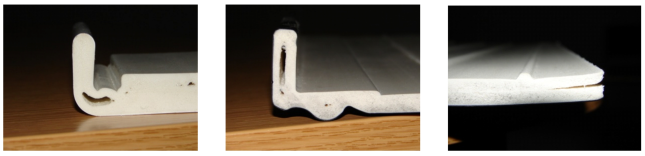

Figure 3: Fascia boards with defaults

board that has a typical density of 0.4-0.8 g/cm^3. The desired degree of foaming can, in principle, be achieved by adjusting the amount of foaming agent used; however, foaming agents are expensive and need to be used sparingly. On the other hand, the use of insufficient amounts of the foaming agent can lead to defaults - these often occur at the corners, where air bubbles can form, or in the central flat part of the board, where the foam layers, as they grow from the top and bottom molten PVC layers, do not join correctly; various types of defect are shown in the three photographs in Figure 3. For later reference, Figure 4 shows the typical foam structure within a manufactured fascia board; evident here is that the pore sizes are much smaller, and the porosity is much less, towards the bottom of the photograph, corresponding to the surface that is cooled directly, than are the pore sizes near the top, which corresponds to the half-width of the board.

In view of the above discussion, it appears most pertinent to study the foaming process in detail, i.e. step 3, since this will determine the ultimate foam structure within the board, and thus whether or not there are defaults; hence, this study will develop a mathematical model for this process, with a view to determining how production parameters should be adjusted, in order to avoid defaults, although without increasing the density of the board. At the outset, it is worth noting that there are comparatively few models in the literature on this type of process, and none on this one in particular; of some use, although limited relevance, are the papers by Choudhary and Kulkarni [1], Leung et al. [3], Potente et al. [4], and Wang et al. [5].

Figure 4: Foam structure: there are comparatively fewer bubbles at the bottom (the cooled surface) than at the top, which is at the half-width.

The outline of this report is as follows. The model equations are presented in §2, and nondimensionalized in §3, with preliminary results being given in §4. In §5, an alternative model is proposed qualitatively. In §6, conclusions are drawn and recommendations for future modelling work are outlined.

2 Modelling

Although the geometry where foaming takes place is three-dimensional, the fundamentals of the process can be demonstrated with a one-dimensional model. The actual geometry of interest is that shown in Figure 2, albeit extruded into the page. If we assume that there is no dependence in the y-direction, then the problem depends only on x and z. Assuming steady-state operation, we see that x effectively acts as a time-like variable. Hence, we can consider a one-dimensional time-dependent model with z as the space variable and t as the time variable, and with x related to t via $x = U_{ext}t$, where U_{ext} is the constant extrusion speed; typically, $U_{ext} \sim 0.02\ \mathrm{ms}^{-1}$. Consequently, the model geometry that we consider is as in Figure 5, which shows a porous foam that occupies $0 < z < s\,(t)$ and whose extent increases with time; ultimately, the foam can occupy $0 < z < h$, where h denotes the half-width of a finished board (see also Figure 2).

The governing equations for $0 < z < s\,(t)$ are then as follows. Conservation of melt gives

$$\frac{\partial}{\partial t}\left(\rho^{(l)}\,(1-\alpha)\right) + \frac{\partial}{\partial z}\left(\rho^{(l)}(1-\alpha)w\right) = 0, \tag{2.1}$$

where $\rho^{(l)}$ is the melt density, α is the gas fraction and w is the z-direction

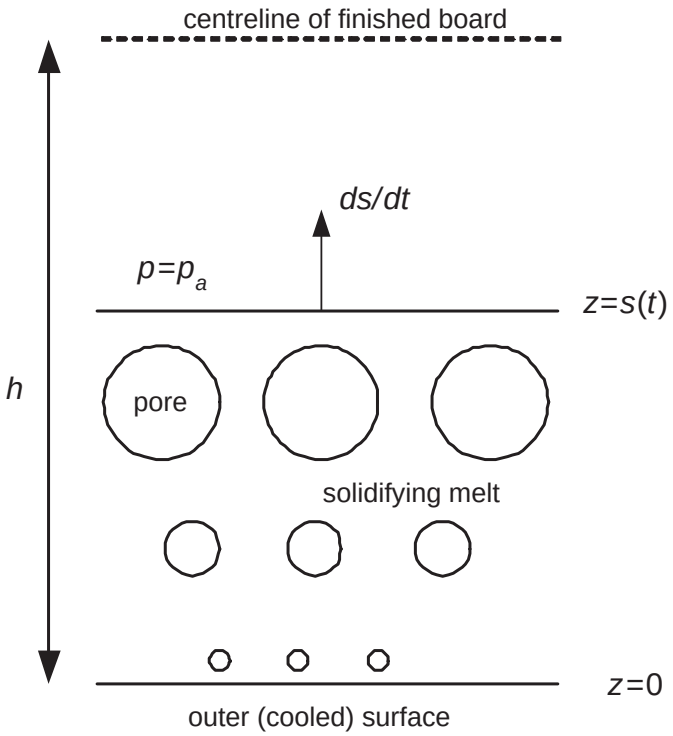

Figure 5: Model schematic

velocity. Conservation of gas gives

$$\frac{\partial}{\partial t}\left(\rho^{(\mathrm{g})}\alpha\right) + \frac{\partial}{\partial z}\left(\rho^{(\mathrm{g})}\alpha w\right) = \frac{D}{d_i^2} M\alpha^{2/3}(c - K_H p), \tag{2.2}$$

where $\rho^{(\mathrm{g})}$ is the gas density, M is the molar mass of the gas, c is the concentration of dissolved gas (mol m^{-3}), p is the gas pressure, K_H is Henry's constant, D is the effective diffusion coefficient for the gas in the melt phase and d_i is the inter-bubble spacing, which is being used here as a diffusion length scale; an alternative would have to use the bubble size as the diffusion length scale, in which case $\alpha^{2/3}$ would have been replaced by $\alpha^{1/3}$. For $\rho^{(\mathrm{g})}$, we use the ideal gas law,

$$\rho^{(\mathrm{g})} = \frac{pM}{RT}, \tag{2.3}$$

where R is the universal gas constant (8.314 J mol^{-1}K^{-1}) and T is the temperature. The term on the right-hand side of equation (2.2) denotes a source term for the production of gas, with the amount of gas produced being proportional to the shift away from Henry's law, i.e. when $c = K_H p$. Conservation of momentum in the z-direction gives

$$\frac{\partial}{\partial z}\left(-p + 2\eta\frac{\partial w}{\partial z}\right) = 0, \tag{2.4}$$

where η is the melt viscosity; typically, η also will be a function that is strongly dependent on temperature, e.g. Arrhenius form. For simplicity, we have taken the melt pressure that appears in equation (2.4) to be same as the gas pressure, p. Equation (2.4) can be integrated once with respect to z to give

$$-p + 2\eta\frac{\partial w}{\partial z} = -p_a, \tag{2.5}$$

where p_a denotes atmospheric pressure. Conservation of dissolved gas in the melt phase gives

$$\frac{\partial}{\partial t}\left((1-\alpha)c\right) + \frac{\partial}{\partial z}\left((1-\alpha)cw\right) = -\frac{D}{d_i^2}\alpha^{2/3}(c - K_H p), \tag{2.6}$$

where c is the dissolved gas concentration; combining with equation (2.2) then gives

$$\frac{\partial}{\partial t}\left(\rho^{(\mathrm{g})}\alpha + M(1-\alpha)c\right) + \frac{\partial}{\partial z}[\left\{\rho^{(\mathrm{g})}\alpha + M(1-\alpha)c\right\} w] = 0. \tag{2.7}$$

Finally, conservation of energy gives

$$\left\{\rho^{(\mathrm{g})}C_p^{(\mathrm{g})}\alpha + \rho^{(\mathrm{l})}C_p^{(\mathrm{l})}(1-\alpha)\right\}\left(\frac{\partial T}{\partial t} + \frac{\partial}{\partial z}(wT)\right) = \frac{\partial}{\partial z}\left(\left[k^{(\mathrm{g})}\alpha + k^{(\mathrm{l})}(1-\alpha)\right]\frac{\partial T}{\partial z}\right), \tag{2.8}$$

where $C_p^{(\mathrm{g})}$ and $C_p^{(\mathrm{l})}$ denotes the specific heat capacities of the gas and melt respectively, and $k^{(\mathrm{g})}$ and $k^{(\mathrm{l})}$ denote the thermal conductivity of the gas and

melt, respectively. Note that there may well be a non-negligible heat source/sink on the right-hand side of equation (2.8), but as we have no way at present to determine its form or magnitude, we omit any further discussion of it; we also neglect any possible frictional heating.

The boundary conditions are: at $z = 0$,

$$T = T_{cold}; \tag{2.9}$$

at $z = s(t)$,

$$T = T_0, \quad w = (1 - \alpha)\frac{ds}{dt}. \tag{2.10}$$

The initial conditions are

$$c = c_0, \quad s = s_0, \quad T = T_0, \quad \alpha = 0, \tag{2.11}$$

where c_0 is the initial dissolved gas concentration and s_0 is the width of the inlet in the z-direction

3 Nondimensionalization

In order to nondimensionalize the equations, we note first that there are three time scales in the problem. These are the viscous time scale t_V, the thermal conduction time scale t_C, and the gas diffusion time scale t_D; they are defined explicitly by

$$t_V = \frac{\eta_0}{p_a}, \quad t_C = \frac{h^2}{\kappa}, \quad t_D = \frac{d_i^2}{D}, \tag{3.1}$$

where η_0 is the viscosity scale and κ is the thermal diffusivity, $k^{(l)}/\rho^{(l)}C_p^{(l)}$. Using values given in Table 1, some of which have been taken from Leung et al. [3], we find

$$t_V \sim 1 \text{ s}, \quad t_C \sim 250 \text{ s}, \quad t_D \sim 10 \text{ s}. \tag{3.2}$$

Symbol	Meaning	Typical value
c_0	initial dissolved gas concentration	10 mol m^{-3}
$C_p^{(g)}$	gas specific heat capacity	800 J $kg^{-1}K^{-1}$
$C_p^{(l)}$	PVC specific heat capacity	900 J $kg^{-1}K^{-1}$
D	effective diffusion coefficient	10^{-9} m^2s^{-1}
d_i	inter-bubble spacing	1×10^{-4} m
h	sample half-width	5×10^{-3} m
$k^{(g)}$	gas thermal conductivity	0.02 $Wm^{-1}K^{-1}$
$k^{(l)}$	PVC thermal conductivity	0.2 $Wm^{-1}K^{-1}$
K_H	Henry's constant	$8.4{\times}10^{-5}$ mol $N^{-1}m^{-1}$
L	length of stainless steel calibrator	0.05-0.1 m
M	molar mass of gas	0.028/0.044 kg mol^{-1} (N_2/CO_2)
p_a	atmospheric pressure	10^5 Pa
s_0	inlet width in the z-direction	1×10^{-3} m
T_{cold}	cooling temperature	300 K
T_0	initial PVC melt temperature	450 K
η_0	viscosity	10^5 Pa s
$\kappa \left(k^{(l)}/\rho^{(l)}C_p^{(l)}\right)$	PVC thermal diffusivity	10^{-7} m^2s^{-1}
ρ_g	gas density	1 kg m^{-3}
$\rho^{(l)}$	PVC density	1000 kg m^{-3}

Table 1: Model parameters

We nondimensionalise by setting

$$\tilde{t} = \frac{t}{t_V}, \quad \tilde{z} = \frac{z}{h}, \quad \tilde{p} = \frac{p}{p_a}, \quad \tilde{s} = \frac{s}{h},$$
$$\tilde{T} = \frac{T}{T_0}, \quad \tilde{w} = \frac{w}{h/t_V}, \quad \tilde{c} = \frac{c}{c_0}, \quad \tilde{\eta} = \frac{\eta}{\eta_0}.$$

Dropping the tildes, we can write the dimensionless equations describing the system in the form

$$p = 1 + 2\eta w_z, \tag{3.3}$$
$$-\alpha_t + [(1-\alpha)w]_z = 0, \tag{3.4}$$
$$T_t + (wT)_z = \frac{1}{Pe} T_{zz}, \tag{3.5}$$
$$\left[\frac{\alpha p}{T} + \lambda(1-\alpha)c\right]_t + \left[\left\{\frac{\alpha p}{T} + \lambda(1-\alpha)c\right\} w\right]_z = 0, \tag{3.6}$$
$$\left(\frac{\alpha p}{T}\right)_t + \left(\frac{\alpha p w}{T}\right)_z = \Lambda \alpha^{2/3}(c - \mu p); \tag{3.7}$$

in order to enable later analytical development, we have used the fact that

$$k^{(g)}/k^{(l)} \ll 1, \quad \rho_g/\rho^{(l)} \ll 1, \quad C_p^{(g)}/C_p^{(l)} \sim 1,$$

where $\rho_g = Mp_a/RT_0$, to simplify equation (2.8) to a form where, on neglecting the $(1-\alpha)$ dependence on both sides, we obtain equation (3.5). The nondimensional parameters in equations (3.3)-(3.7) are defined by

$$Pe = \frac{t_C}{t_V} \sim 250, \quad \lambda = \frac{Mc_0}{\rho_g} \sim O(1), \quad \Lambda = \frac{\lambda t_V}{t_D} \sim 0.1, \quad \mu = \frac{K_H p_a}{c_0} \sim 0.1. \tag{3.8}$$

It follows from these, that since $c = 1$, $\alpha = 0$, $p = 1$ at $t = 0$, then

$$c = 1 - \frac{\alpha p}{\lambda T(1-\alpha)}. \tag{3.9}$$

With $\Lambda \ll 1$, it is appropriate to rescale the variables by putting

$$p = 1 + \Lambda P, \quad w \sim \Lambda, \quad t \sim \frac{1}{\Lambda}, \tag{3.10}$$

and with this the equations can be approximated as

$$\alpha_t + w\alpha_z = (1-\alpha)\, w_z, \tag{3.11}$$

$$T_t + (wT)_z = \frac{1}{Pe} T_{zz}, \tag{3.12}$$

$$\left(\frac{\alpha}{T}\right)_t + \left(\frac{\alpha w}{T}\right)_z = \alpha^{2/3}\left(1 - \mu - \frac{\alpha}{\lambda(1-\alpha)T}\right). \tag{3.13}$$

The Péclet number $Pe \sim 250$ is large, and the temperature will be isothermal, thus $T \approx 1$, except in a thin thermal boundary layer near the base $z = 0$, and with this assumption, the model reduces to

$$\alpha_t + (w\alpha)_z = g(\alpha) \equiv \alpha^{2/3}\left(1 - \mu - \frac{\alpha}{\lambda(1-\alpha)}\right) = w_z, \tag{3.14}$$

together with

$$\alpha = 0 \quad \text{at} \quad t = 0, \quad w = 0 \quad \text{on} \quad z = 0. \tag{3.15}$$

The solution is $\alpha = \alpha(t)$ given by

$$t = \int_0^\alpha \frac{d\alpha}{g(\alpha)}, \tag{3.16}$$

and then it follows from the kinematic condition at $z = s(t)$ that

$$\dot{s} = \frac{g(\alpha)s}{1-\alpha}; \tag{3.17}$$

together with $s = s_0$ at $t = 0$ ($s_0 \approx 0.2$), we find $s = s_0/(1-\alpha)$, and the maximum thickness of the half-width foam layer is

$$s_{\max} = s_0[1 + \lambda(1-\mu)]. \tag{3.18}$$

Values of $\lambda \gtrsim 5$ lead to filling of the interior with foam, as desired.

However, the above does not take into account the effect of cooling; in reality, the temperature in the developing foam is not uniform, because of the application of a cooling temperature at the exterior surface of the foam, i.e. $z = 0$. Because the Péclet number is relatively high, it is appropriate to rescale the variables in a boundary layer adjoining the base, and we therefore write

$$z = \frac{Z}{\sqrt{Pe}}, \quad w = \frac{W}{\sqrt{Pe}}, \tag{3.19}$$

and equations (3.11)-(3.13) then become

$$\alpha_t + W\alpha_Z = (1-\alpha)\,W_Z, \tag{3.20}$$

$$T_t + (WT)_Z = T_{ZZ}, \tag{3.21}$$

$$\left(\frac{\alpha}{T}\right)_t + \left(W\frac{\alpha}{T}\right)_Z = \alpha^{2/3}\left(1 - \mu - \frac{\alpha}{\lambda(1-\alpha)T}\right), \tag{3.22}$$

respectively; they are supplemented by the conditions

$$\alpha = 0, \quad T = 1 \quad \text{at } t = 0, \tag{3.23}$$

$$W = 0, \quad T = 0 \quad \text{at } Z = 0. \tag{3.24}$$

4 Results

In general, these equations require numerical solution, but a simplification ensues when we apply the condition that W decreases at low temperatures due to the rapid increase of viscosity at lower temperatures. A simple formulation of this prescribes $W = 0$ when $T < T^*$, and then the temperature simply satisfies the diffusion equation for $T < T^*$. If T^* is close to 1, as is reasonable since the viscosity varies strongly with temperature, then we have approximately

$$T \approx \operatorname{erf}\left(\frac{Z}{2\sqrt{t}}\right), \tag{4.1}$$

while the outer solution can be applied for $T > T^*$. If we define ζ^* by

$$\operatorname{erf}\zeta^* = T^*, \tag{4.2}$$

then the outer solution applies for

$$z > z_f = \frac{2\zeta^*\sqrt{t}}{\sqrt{Pe}}, \tag{4.3}$$

with, however, $w = 0$ on $z = z_f$; a qualitative schematic of the temperature profile through a cross-section of the board is given in Figure 6.

Solving the equations as before leads to the prescription for the foam boundary,

$$\dot{s} = \left[s - \frac{2\zeta^*\sqrt{t}}{\sqrt{Pe}}\right]\frac{g(\alpha)}{1-\alpha},$$

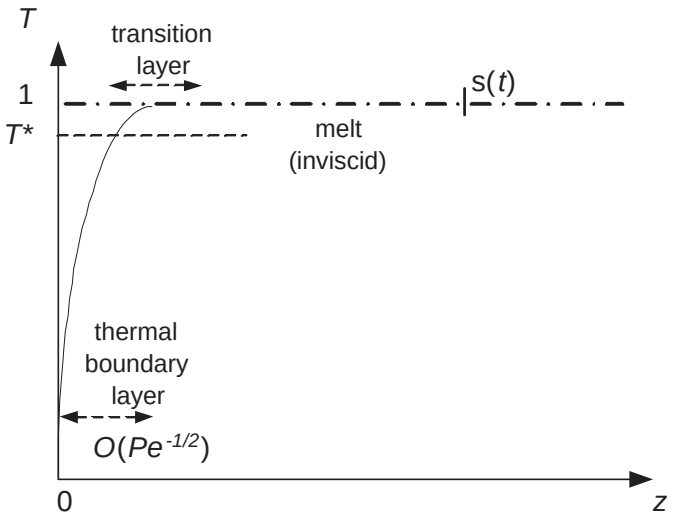

Figure 6: Qualitative schematic of the temperature profile through a cross-section of the board

with α still given by (3.16). A plot of this is given in Figure 7, and shows that α rapidly approaches a steady state value of $\lambda(1-\mu)/(1+\lambda(1-\mu)) \approx 0.47$. The evolution of s with t for different values of ζ^* is given in Figure 8 and the variation of $s(\infty)$ with ζ^* is shown in Figure 9. The latter shows that the maximum foam penetration is sensitively dependent on the value of ζ^*: thus, cooling has a significant effect on the foaming process.

5 Discussion

In the above, the gases (N_2 or CO_2) were assumed to be already dissolved within the pressurized molten PVC; pressure release leads to the exsolution of the gases. Consequently, the above model is only able indirectly, via the prescription of c_0, to take account of what would happen if the amount of foaming agent used were changed. Hence, the model does not take into account how much foaming agent is actually present, or how much gas it is able to produce.

However, there is an alternative interpretation as to what happens. An alternative model would append a conservation equation for the concentration of foaming agent and would explicitly model its consumption; furthermore, one would not need to assume that there was any dissolved gas at all prior to exit from the extruder. Although we do not write down corresponding equations for this model here, it is evident that, qualitatively at least, a similar conclusion to that of the first model will be obtained. First of all, if the temperature were uni-

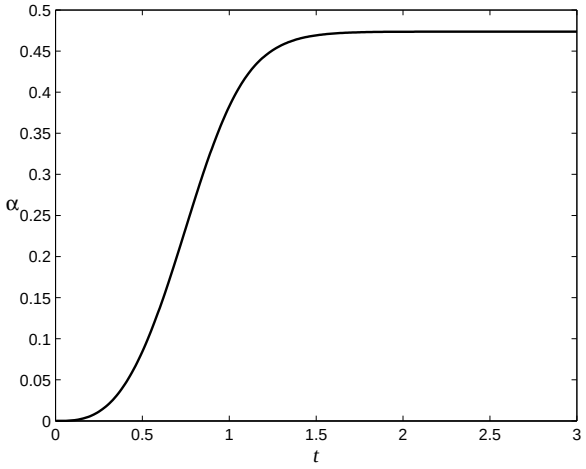

Figure 7: α vs. t

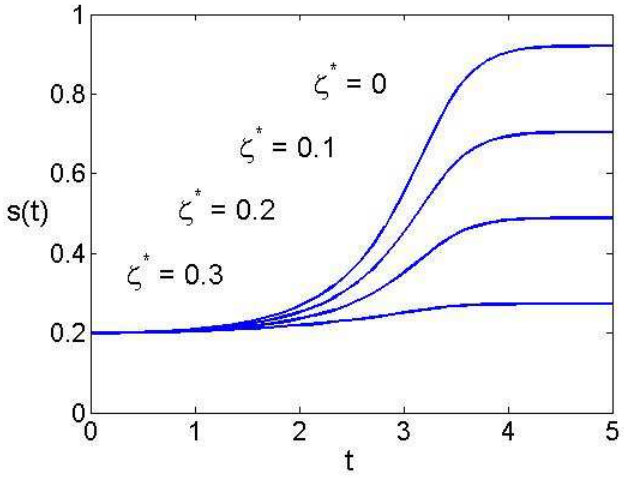

Figure 8: s vs. t for different values of ζ^*; the curves, uppermost to lowermost, are for increasing values of ζ^*.

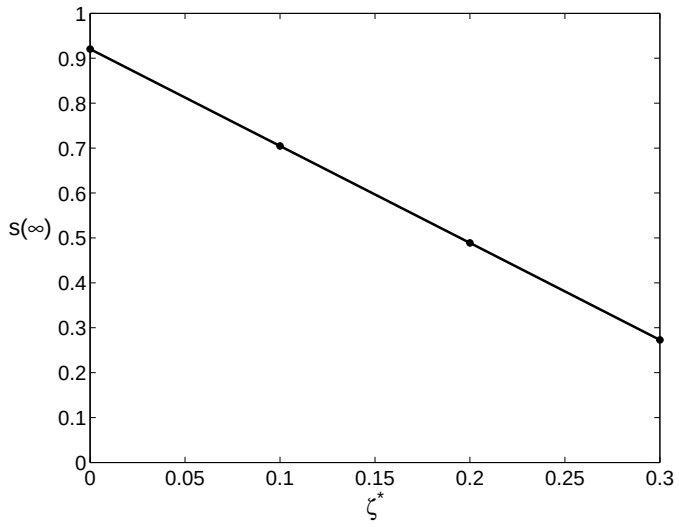

Figure 9: $s\,(\infty)$ vs. ζ^*

form across the cross-section, i.e. at around 450 K, then the temperature would be sufficiently high everywhere for the foaming agent to decompose throughout and to produce gas. In practice, the temperature is not uniform, but is much lower near $z = 0$. Consequently, this will mean that the gas-producing reaction will proceed very slowly, if at all, near $z = 0$, resulting in unspent foaming agent, as well as a denser foam, since comparatively little gas is produced there. These comments appear to tie in with *ad hoc* observations that not all of the foaming agent is consumed in the process, as well as with the foam structure shown in Figure 4. Of course, what exactly happens is open to speculation, in view of the complexities associated with the foaming agents: the N_2-producing foaming agent is, by itself stable at 450 K, but requires additives to activate it at temperatures lower than this, whereas the CO_2-producing foaming agent reacts at temperatures as low as 400 K; the N_2-producing foaming agent decomposes more quickly than the CO_2-producing foaming agent; and the latter produces a coarser cell structure than the former.

6 Conclusions

The aim of this report has been to develop a mathematical model that explains the formation of undesired voids that occur during the manufacture of PVC fascia boards. Although the overall process consists of several steps, the key one appears to be the foaming process, during which a pressurized mixture of molten PVC and foaming agents are extruded through a die that is shaped in

the exterior of a board; subsequent pressure release triggers foaming, so that the interior of the board is filled, simultaneously as the board is cooled. Two alternative interpretations were considered:

1. the pressure release enables gases that were already dissolved in the molten PVC to exsolve, thereby creating the foam;

2. the pressure release enables the foaming agents to react and produce gas.

In the first case, the fact that the board is being cooled at one surface means that there is a thermal boundary layer there, in which the viscosity is high, so that there is little expansion there; this results in a board with a void. In the second case, the self-same thermal boundary layer means that the foaming reaction cannot occur there as desired, since the temperature is lower than that required for the foaming agents to decompose; consequently, foaming agent goes unused, once again resulting in a board with a void in its centre. In either case, it is evident that the strong temperature dependence of both the viscosity and the reaction rate are decisive: a 5 K decrease in temperature roughly doubles the viscosity and halves the reaction rate (Collins [2]).

Specific recommendations for future theoretical work would be to:

- develop further the 1D time-dependent model for case 1 that was initiated here - there still remain uncertainties about parameter values and the actual temperature dependence of both the viscosity and the reaction rate;

- develop a parallel model for case 2;

- consider the possible effect of the heat of reaction which, whilst not affecting the homogeneity of the temperature, will affect the temperature as function of time;

- continue to exploit possible simplifications through scaling and nondimensionalization, as has already been shown for case 1.

Once such models have been derived, they can be extended to at least 2D, to describe more realistically what actually happens at corners, which is where the most serious voids appear to occur.

Acknowledgements

A. C. Fowler, W. T. Lee, S. L. Mitchell and M. Vynnycky acknowledge the support of the Mathematics Applications Consortium for Science and Industry (www.macsi.ul.ie) funded by the Science Foundation Ireland Mathematics Initiative Grant 06/MI/005.

References

[1] Choudhary, M. K. and Kulkarni, J. A., Modeling of three-dimensional flow and heat transfer in polystyrene foam extrusion dies, *Polymer Engineering and Science* **48** (2008), 1177-1188.

[2] Collins, E. A., The rheology of PVC - an overview, *Pure and Applied Chemistry* **49** (1977), 591-595.

[3] Leung, S. N., Park, C. B., Xu, D., Li, H. and Fenton, R. G., Computer simulation of bubble-growth phenomena in foaming, *Industrial & Engineering Chemistry Research* **45** (2006), 7823-7831.

[4] Potente, H., Moritzer, E. and Obermann, Ch., Foam formation in gas-assisted injection molded parts: theoretical and experimental considerations, *Polymer Engineering and Science* **36** (1996), 2163-2171.

[5] Wang, L., Ganjyal, G. M., Jones, D. D., Weller, C. L. and Hanna, M. A., Modeling of bubble growth dynamics and nonisothermal expansion in starch-based foams during extrusion, *Advances in Polymer Technology* **24**:1 (2005), 29-45.